

Development of an analysis method for neutrino-induced air showers with the Telescope Array surface detectors

K.Takahashi,^{a,*} T.Sako,^a K.Fujisue,^b K.Fujita,^a K.Kawata,^a S.Ogio,^a H.Oshima,^a H.Sagawa^a and M.Takeda^a for the Telescope Array collaboration

^a*ICRR, the University of Tokyo,*

5-1-5 Kashiwa-no-Ha, Kashiwa City Chiba, 277-8582, Japan

^b*Institute of Physics, Academia Sinica,*

No.128, Sec.2, Academia Rd., Taipei 115, Taiwan

E-mail: ktakaha4@icrr.u-tokyo.ac.jp

The origins of Ultra High Energy Cosmic Rays (UHECRs) remain unclear. A significant difficulty in identifying their sources is the complex deflection of charged particles by galactic and intergalactic magnetic fields. Our goal is to detect high-energy neutrinos produced through interactions between UHECRs and matter near astrophysical objects, to help elucidate their origins. In this study, we utilize data from the Telescope Array surface detector (TA SD) to search for neutrino-induced air showers. To achieve this, we have developed an analysis method using Monte Carlo (MC) simulations. Our approach focuses on inclined air showers, as both the probability of interaction and the efficiency of background rejection increase at larger zenith angles. Since standard TA analyses limit zenith angles below 55 degrees, this study rigorously examines the validity of thinning and dethinning processes in MC simulations at larger zenith angles. To minimize variations in shower characteristics, we concentrate on showers produced by electron neutrinos through charged current interactions. This study will not only present a detailed analysis method but also discuss the characteristics of neutrino-induced air showers, which are essential for distinguishing them from background events.

*7th International Symposium on Ultra High Energy Cosmic Rays (UHECR2024)
17-21 November 2024
Malargüe, Mendoza, Argentina*

*Speaker

1. Introduction

Highest energy cosmic rays have been studied by the Telescope Array experiment (TA) and the Pierre Auger observatory (Auger), which operate in the Northern and Southern hemisphere, respectively [1], [2]. These experiments indicate medium scale anisotropy of cosmic-ray arrival direction at extremely high energies. UHECRs are believed to be of extragalactic origin. Since cosmic rays are charged particles, it is difficult to identify the source because their trajectories are bent by magnetic fields. It is well known that observation of neutrino is useful to identify origins of UHECRs because neutrinos are not affected by magnetic fields. In this paper, performance of the TA Surface Detector (SD) array for neutrino-induced air showers is discussed. We focus on the large zenith angle region to increase the probability of interaction with atmosphere. Furthermore, at large zenith angles, the first interaction points of the background (BG) hadron-induced showers and the neutrino-induced showers are significantly different, resulting in a difference in the shape of the shower front. This makes it easier to discriminate neutrinos from BGs than at small zenith angles.

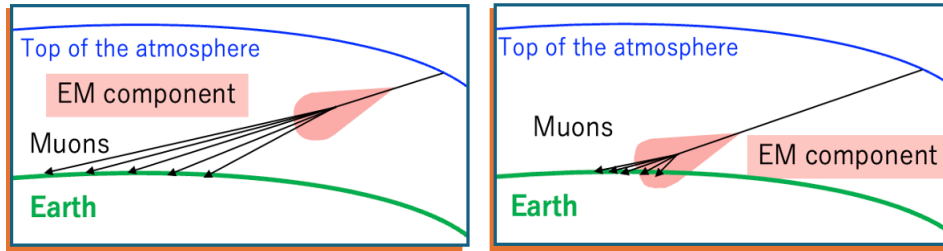


Figure 1: Schematic view of inclined showers

A visual representation of a proton shower and a neutrino shower at a large zenith angle is presented in Fig.1. For large zenith angles, BG hadron showers interact in the upper atmosphere, resulting in a predominant population of muons among the particles reaching the Earth's surface. In contrast, neutrino showers, even at large zenith angles, can begin to develop near the Earth's surface, leading to a significant electromagnetic component in their early interaction stages. Consequently, the shape of the shower front differs between hadron showers, which are flat, and neutrino showers, which are predicted to exhibit a curved surface with a smaller curvature radius.

The TA collaboration have investigated large zenith angle region to search ultra-high energy neutrinos [3]. We discriminated neutrino-induced showers from proton-induced showers using machine learning method called Boosted Decision Trees [4], [5]. We used large zenith angle Monte Carlo (MC) data and define the optimum parameter. The method of this analysis was applied to the TA data and no neutrino candidate events were found. The previous study explored diffuse neutrino and did not need to increase the accuracy of angular resolution, so it was not validated to the MC data generation method. However, the objective of this study is to search for an astrophysical neutrino, and all steps from the shower generation method to the reconstruction method need to be verified. In this paper, we'll mainly focus on MC generation of the neutrino inclined showers. Thinning by CORSIKA and De-thinning by TA method for inclined neutrino showers will be discussed. We also discuss about discrimination method between neutrino and proton, using MC data generated by

new method for inclined neutrino showers.

2. Telescope Array Experiment

The TA experiment is the largest cosmic ray observatory in the Northern Hemisphere, located at 113° W longitude and 39° N latitude in the desert of Utah, USA. It observes the highest energy cosmic rays at an altitude of 1430 m (875 g/cm^2 mass-overburden). The 507 surface detectors are installed at 1.2 km intervals, covering approximately 700 km^2 . The TA experiment started observations in 2008 and has been in operation since then.

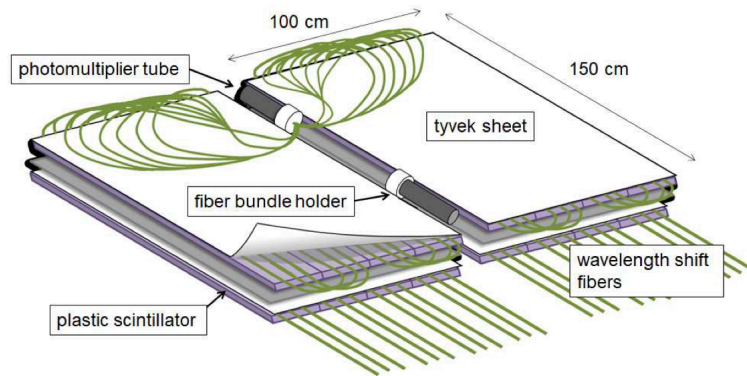


Figure 2: Telescope Array Experiment surface detector

Each SD consists of two layers of 3m^2 scintillators as shown in Fig.2. The lights emitted by these scintillators are converted to electrical signals by photomultiplier tubes (PMT) and recorded as waveforms. The standard analysis of the TA experiment is optimized for zenith angles below 55° . By our study, we aim to evaluate the reconstruction method for the larger zenith angle region by utilizing MC data.

3. Monte Carlo generation of inclined neutrino showers

3.1 Thinning and De-thinning process

In MC of air showers, "Thinning" is performed to reduce the number of tracked particles by weighting representative particles instead of following all secondary particles in the shower. Then, "Dethining" is also performed, which recovers the number of particles according to the weights as shown in Fig.3. In this study, We worked on optimizing the Dethining method developed in the TA for showers created in the Thinning mode of CORSIKA so that it can be applied to neutrino large zenith angle showers as well. Specifically, we first compared the energy at which secondary particles are deposited on the SD, the arrival time, and the number of particles hitting the SD for the case where all secondary particles were tracked (Unthinned) and the case where Thinning-Dethinning was used for the same shower (Dethinned). We will report the results and the improvement of the Dethinning method.

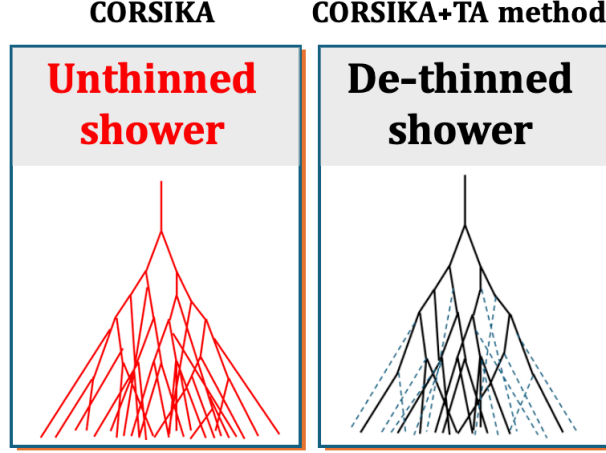


Figure 3: Schematic view of Unthinned/Dethinned showers

3.2 MC dataset and CORSIKA setup

For the verification of the dethinning method, we used CORSIKA MULTITHIN option. Using this option, we can generate Nothinning shower and Thinning shower simultaneously. By comparing exactly the same showers, we can reduced the number of simulation events. The MC dataset is shown in Table 1.

Table 1: Neutrino MC dataset: 1st interaction for all showers is Charged Current.

Particle Type	Energy [eV]	Zenith Angle [deg]	Azimuth Angle [deg]	1st interaction height [km]
ν_e	$10^{17}/10^{18}/10^{19}$	70/80	0 to 360	3,5,7

In this paper, we investigated only showers generated through Charged Current (CC) interaction by high energy ν_e and atmosphere.

4. Comparison of Unthinned and Dethinned showers

4.1 Calculation setup and how to compare

We simulate the response of a virtual array filled with $6 \text{ m} \times 6 \text{ m}$ tiles. One $3 \text{ m} \times 3 \text{ m}$ TA SD is placed in the center of each tile, arranged in a $16.8 \text{ km} \times 16.8 \text{ km}$ area, and the response of each tile is calculated.

The example of the distrubution of deposited energy over the vertual array is shown in right of the Fig.4.

We compared three parameters here, number of particles, energy deposit and arrival timing. We compared each parameters projected onto the vector projecting the shower axis onto the ground and calculated the ratio as $P = \int \text{Dethenned} / \int \text{Unthinned}$. P was calculated for 18 showers as shown in Table 1.

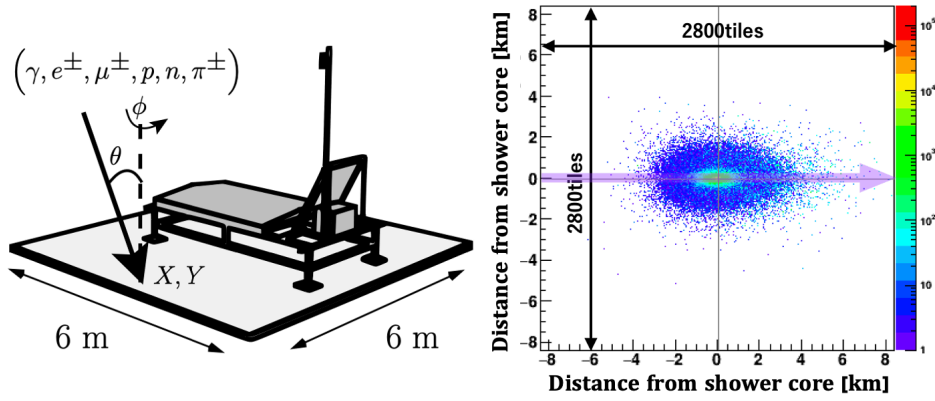


Figure 4: Energy deposit calculation setup

Fig.5 shows comparison of the number of particles for each energies. The right figure shows the results of the calculation of P for the number of particles for a 70 deg shower, and the left figure shows the results for an 80 deg shower. From Fig.5, we can see that Dethinned showers underproduce particles compared to Unthinned showers, both at 70 deg and at 80 deg. In investigating the cause of this difference, we found that it is attributable to the electromagnetic component.

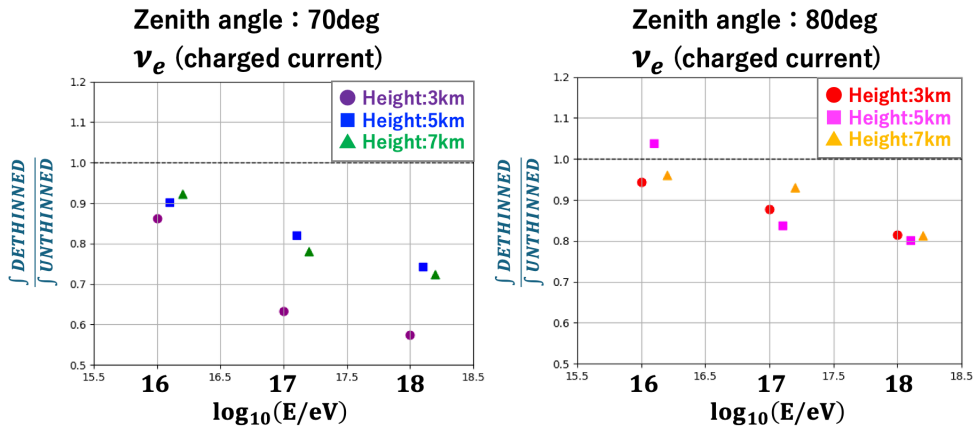


Figure 5: Number of particles before modification

We tuned for W_{rate} , the maximum number of particles that can be represented by THINNING, for the electromagnetic component in CORSIKA shower generation. The original method, upper weight limit on the electromagnetic component can be up to 100 times higher than the hadronic component. $W_{rate} = WMAX_{em}/WMAX_{had} = 100$ After modification, we tuned like $W_{rate} = WMAX_{em}/WMAX_{had} = 1$, so the maximum weight for electromagnetic component has been decreased. The CPU time doubles after modification, but it's still acceptable. The Fig.6 shows that the comparison of the number of particles after modification.

It can be observed that there is good agreement across all energies and interaction heights, with differences remaining within $\pm 1\%$. Regarding the total energy deposit and average arrival timing, the initial agreement was reasonably good; however, after modification, the distribution has further

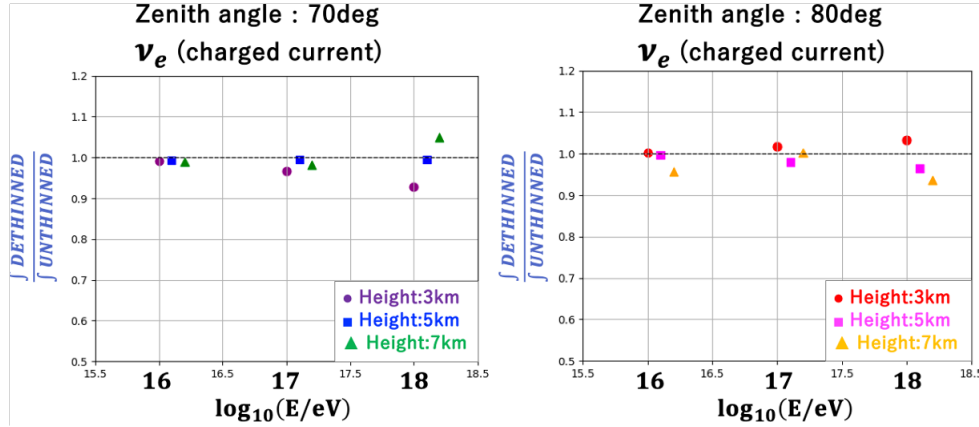


Figure 6: Number of particles after modification

improved, achieving nearly 100% agreement.

5. For discrimination between neutrino and proton showers

Here, we also discuss about the discrimination parameters between neutrino from proton showers. Table 2 shows the MC setup used to investigate the discrimination parameters.

Table 2: Neutrino MC dataset for discrimination

Particle Type	Energy [eV]	Zenith Angle [deg]	Azimuth Angle [deg]	1st interaction height [km]
ν_e	10^{18}	70/80	0 to 360	3,4,5,6,7,8
Proton	$10^{18.5}/10^{19}/10^{19.5}/10^{20}/10^{20.5}$	70/80	0 to 360	

Here the neutrino shower energy is only 10^{18} eV, but this will be extended in the future. Each bin was filled with 30 showers each, producing a total of 360 showers for neutrinos and 300 showers for proton. CORSIKA showers were reused an average of 8000 times by re-swinging the core position in a random within a 25 km radius circle containing the TA SD array. Two parameters were investigated in this paper. Area Over Peak (AoP), the Peak value of the waveform divided by Area, and curved parameter a , one of the shower surface fit parameters. AoP was chosen because of the difference in the typical waveforms included in neutrino inclined showers and proton inclined showers. For neutrino inclined showers, the shower has much electromagnetic component and the AoP is relatively large when the 1st interaction height is low. On the other hand, for proton inclined showers, there are many muons and the AoP is relatively small since the shower runs a long distance to reach the ground. Here, the AoPs of all waveforms in the shower are calculated and averaged for each of the upper and lower scintillators. Thus, the AoP is calculated one per shower. We chose curved parameter a because of the difference between the neutrino and proton shower surfaces. Neutrino inclined showers that have low 1st interaction point have a small curvature radius. It means shower fronts are curved and a become large. Proton inclined showers that have high 1st interaction point have a large curvature radius. It means shower fronts are flat and a become small. Because of this property, we can distinguish between the two.

Fig.7 shows the result of discrimination using those two parameters.

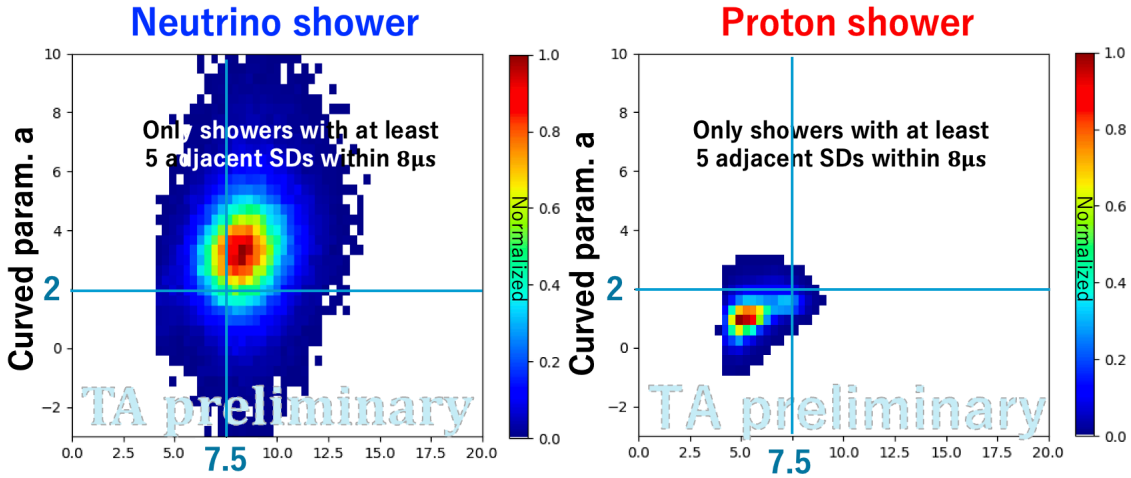


Figure 7: Relation between two discrimination parameters. X-axis represents to average AoP and Y-axis represents to curved parameter a. Left figure is for neutrino showers and right figure is for proton showers. The blue lines in the figure are just landmark to compare two figures, and they don't have particular meaning.

We can see the trend that neutrino showers have large values for both AoP and curved parameter a, while Proton showers have small ones relatively. AoP and curved parameter a seemed to be available for discrimination.

6. Summary and prospects

In this paper, the dethinning method for large zenith angle neutrino showers was verified. We found that the agreement is particularly poor for the electromagnetic component. We tuned W_{rate} for electromagnetic component and the maximum weight has been decreased. After the modification, the agreement of number of particles become better and difference between Unthinned and Dethinned shower become within $\pm 10\%$. For total energy deposit and average arrival timing, the distribution has further improved to near 100% agreement after modification. In the discussion on discrimination methods, observational parameters for neutrinos and protons in the large zenith angle region are compared. We found that AoP and curved parameter a seemed to be available for discrimination. The application of current reconstruction methods to neutrino showers is currently being investigated and studied. Previous analysis has shown that neutrino-inclined showers have a tendency to estimate the zenith angle smaller. This is due to the asymmetry of the shower surface. On the other hand, the azimuth angle is well determined. Further analysis will be conducted to develop a reconstruction method tuned to neutrino showers. In near future, we complete the investigating the analysis methods for inclined neutrino showers and search for neutrinos by observed data TA SD.

References

- [1] The Pierre Auger Collaboration. “ Observation of a Large-scale Anisotropy in the Arrival Directions of Cosmic Rays above 8×10^{18} eV ” . In: SCIENCE (6357 Sept. 2017), pp. 1266–1270. DOI: 10.1126/science.aan4338.
- [2] K. Kawata et al. “ Updated Results on the UHECR Hotspot Observed by the Telescope Array Experiment ” . In: Proceedings of ICRC2019 (2020). DOI: 10.22323/1.358.0310.
- [3] R.U Abbasi TA collaboration. Journal of Experimental and Theoretical Physics 131 2, pp.255-264 (2020)
- [4] L. Breiman et al., Wadsworth International Group (1984)
- [5] R.E. Schapire, Mach. Learn. 5 (1990) 197.

Full Authors List: The Telescope Array Collaboration



R.U. Abbasi¹, T. Abu-Zayyad^{1,2}, M. Allen², J.W. Belz², D.R. Bergman², I. Buckland², W. Campbell², B.G. Cheon³, K. Endo⁴, A. Fedynitch^{5,6}, T. Fujii^{4,7}, K. Fujisue^{5,6}, K. Fujita⁵, M. Fukushima⁵, G. Furlich², Z. Gerber², N. Globus^{8*}, W. Hanlon², N. Hayashida⁹, H. He^{8†}, K. Hibino⁹, R. Higuchi⁸, D. Ikeda⁹, T. Ishii¹⁰, D. Ivanov², S. Jeong¹¹, C.C.H. Jui², K. Kadota¹², F. Kakimoto⁹, O. Kalashev¹³, K. Kasahara¹⁴, Y. Kawachi⁴, K. Kawata⁵, I. Kharuk¹³, E. Kido⁸, H.B. Kim³, J.H. Kim², J.H. Kim^{2‡}, S.W. Kim^{11§}, R. Kobo⁴, I. Komae⁴, K. Komatsu¹⁵, K. Komori¹⁶, C. Koyama⁵, M. Kudenko¹³, M. Kuroiwa¹⁵, Y. Kusumori¹⁶, M. Kuznetsov^{13,17}, Y.J. Kwon¹⁸, K.H. Lee³, M.J. Lee¹¹, B. Lubasandorzhiev¹³, J.P. Lundquist^{2,19}, A. Matsuzawa¹⁵, J.A. Matthews², J.N. Matthews², K. Mizuno¹⁵, M. Mori¹⁶, M. Murakami¹⁶, S. Nagataki⁸, M. Nakahara⁴, T. Nakamura²⁰, T. Nakayama¹⁵, Y. Nakayama¹⁶, T. Nonaka⁵, S. Ogio⁵, H. Ohoka⁵, N. Okazaki⁵, M. Onishi⁵, A. Oshima²¹, H. Oshima⁵, S. Ozawa²², I.H. Park¹¹, K.Y. Park³, M. Potts², M. Przybylak²³, M.S. Pshirkov^{13,24}, J. Remington^{2¶}, C. Rott^{2,11}, G.I. Rubtsov¹³, D. Ryu²⁵, H. Sagawa⁵, N. Sakaki⁵, R. Sakamoto¹⁶, T. Sako⁵, N. Sakurai⁵, S. Sakurai⁴, D. Sato¹⁵, S. Sato¹⁶, K. Sekino⁵, T. Shibata⁵, J. Shikita⁴, H. Shimodaira⁵, B.K. Shin²⁵, H.S. Shin^{4,7}, K. Shinozaki²⁶, J.D. Smith², P. Sokolsky², B.T. Stokes², T.A. Stroman², Y. Takagi¹⁶, K. Takahashi⁵, M. Takeda⁵, R. Takeishi⁵, A. Taketa²⁷, M. Takita⁵, Y. Tameda¹⁶, K. Tanaka²⁸, M. Tanaka²⁹, S.B. Thomas², G.B. Thomson², P. Tinyakov^{13,17}, I. Tkachev¹³, T. Tomida¹⁵, S. Troitsky¹³, Y. Tsunesada^{4,7}, S. Udo⁹, F. Urban³⁰, I.A. Vaiman^{13||}, M. Vrabel²⁶, D. Warren⁸, K. Yamazaki²¹, Y. Zhezher^{5,13}, Z. Zundel², and J. Zvirzdin²

¹ Department of Physics, Loyola University Chicago, Chicago, Illinois 60660, USA

² High Energy Astrophysics Institute and Department of Physics and Astronomy, University of Utah, Salt Lake City, Utah 84112-0830, USA

³ Department of Physics and The Research Institute of Natural Science, Hanyang University, Seongdong-gu, Seoul 426-791, Korea

⁴ Graduate School of Science, Osaka Metropolitan University, Sugimoto, Sumiyoshi, Osaka 558-8585, Japan

⁵ Institute for Cosmic Ray Research, University of Tokyo, Kashiwa, Chiba 277-8582, Japan

⁶ Institute of Physics, Academia Sinica, Taipei City 115201, Taiwan

⁷ Nambu Yoichiro Institute of Theoretical and Experimental Physics, Osaka Metropolitan University, Sugimoto, Sumiyoshi, Osaka 558-8585, Japan

⁸ Astrophysical Big Bang Laboratory, RIKEN, Wako, Saitama 351-0198, Japan

⁹ Faculty of Engineering, Kanagawa University, Yokohama, Kanagawa 221-8686, Japan

¹⁰ Interdisciplinary Graduate School of Medicine and Engineering, University of Yamanashi, Kofu, Yamanashi 400-8511, Japan

¹¹ Department of Physics, Sungkyunkwan University, Jang-an-gu, Suwon 16419, Korea

¹² Department of Physics, Tokyo City University, Setagaya-ku, Tokyo 158-8557, Japan

¹³ Institute for Nuclear Research of the Russian Academy of Sciences, Moscow 117312, Russia

¹⁴ Faculty of Systems Engineering and Science, Shibaura Institute of Technology, Minato-ku, Tokyo 337-8570, Japan

¹⁵ Academic Assembly School of Science and Technology Institute of Engineering, Shinshu University, Nagano, Nagano 380-8554, Japan

¹⁶ Graduate School of Engineering, Osaka Electro-Communication University, Neyagawa-shi, Osaka 572-8530, Japan

¹⁷ Service de Physique Théorique, Université Libre de Bruxelles, Brussels 1050, Belgium

¹⁸ Department of Physics, Yonsei University, Seodaemun-gu, Seoul 120-749, Korea

¹⁹ Center for Astrophysics and Cosmology, University of Nova Gorica, Nova Gorica 5297, Slovenia

²⁰ Faculty of Science, Kochi University, Kochi, Kochi 780-8520, Japan

²¹ College of Science and Engineering, Chubu University, Kasugai, Aichi 487-8501, Japan

²² Quantum ICT Advanced Development Center, National Institute for Information and Communications Technology, Koganei, Tokyo 184-8795, Japan

²³ Doctoral School of Exact and Natural Sciences, University of Lodz, Lodz, Lodz, 90-237, Poland

²⁴ Sternberg Astronomical Institute, Moscow M.V. Lomonosov State University, Moscow 119991, Russia

²⁵ Department of Physics, School of Natural Sciences, Ulsan National Institute of Science and Technology, UNIST-gil, Ulsan 689-798, Korea

²⁶ Astrophysics Division, National Centre for Nuclear Research, Warsaw 02-093, Poland

²⁷ Earthquake Research Institute, University of Tokyo, Bunkyo-ku, Tokyo 277-8582, Japan

²⁸ Graduate School of Information Sciences, Hiroshima City University, Hiroshima, Hiroshima 731-3194, Japan

²⁹ Institute of Particle and Nuclear Studies, KEK, Tsukuba, Ibaraki 305-0801, Japan

³⁰ CEICO, Institute of Physics, Czech Academy of Sciences, Prague 182 21, Czech Republic

* Presently at: KIPAC, Stanford University, Stanford, CA 94305, USA

† Presently at: Purple Mountain Observatory, Nanjing 210023, China

‡ Presently at: Physics Department, Brookhaven National Laboratory, Upton, NY 11973, USA

§ Presently at: Korea Institute of Geoscience and Mineral Resources, Daejeon, 34132, Korea

¶ Presently at: NASA Marshall Space Flight Center, Huntsville, Alabama 35812, USA

|| Presently at: Gran Sasso Science Institute, 67100 L'Aquila, L'Aquila, Italy